Struct Chem (2007) 18:477–491
DOI 10.1007/s11224-007-9167-9

ORIGINAL PAPER

Molecular van der Waals symmetry affecting bulk properties of condensed phases: melting and boiling points

Yuri L. Slovokhotov · Andrei S. Batsanov · Judith A. K. Howard

Published online: 28 April 2007
© Springer Science+Business Media, LLC 2007

Abstract Qualitative analysis of the trends in melting temperatures T_m and boiling temperatures T_b of organic compounds and related substances supports a concept of van der Waals symmetry suggested earlier by the authors. Data for substituted methanes, ethanes, ethylenes, benzenes and cyclohexanes, reveal linear T_b versus M^{α} patterns but usually non-uniform T_m versus M^{α} patterns (where M is the molecular mass, α varies from 0.5 to 1). In the same set of isomers, T_m and T_b often change in different succession. To explain the observed trends, a local van der Waals field U that acts on a molecule in a solid or liquid phase, was represented by a sum of an averaged long-range field U_0 from all molecules, and a short-range ''contact'' term W determined by a molecular shape. Variations of T_m and T_b among closely related substances correspond to different strength of perturbation of $U_0^{(C)}$ (in a crystal) and $U_0^{(L)}$ (in a liquid) by W. Higher T_b of isomers with medium-symmetry molecules (like 1,2-disubstituted benzenes and cyclohexanes) reflect the better fitting of their molecules to a local molecular environment in a liquid (that contains vacancies). Highly symmetrical quasispherical molecules (e.g., C_2Cl_6 or C_6F_{12}) produce a stabilised solid and destabilised liquid state, hence their molecular crystals easily sublime rather than melt at ambient pressure.

Keywords Boiling point · Melting point · Molecular condensed phases · Symmetry

''A molecule has a body''
Alexander I. Kitaigorodskii

Introduction

Bulk properties of molecular substances obviously depend on the structure (atomic connectivity) and related parameters (dipole moment, polarisability, etc.) of the molecules. However, at the moment both the mathematical form of this dependence and the underlying physical effects are understood imperfectly and require further investigations. Recently, a number of empirical correlations between chemical/biological activity of substances and their molecular structure have been elucidated using molecular descriptors [1], but theoretical substantiation of this method is still lacking.

Among physical constants accurately determined for large number of organic and inorganic substances are melting points (mp, or T_m) and boiling points (bp, or T_b). Some intriguing regularities, e.g., alteration of mp in even and odd *n*-alkanes, non-uniform variations of mp among isomers, easy sublimation of compounds with high-symmetric quasispherical molecules, etc., have been empirically known, but not theoretically explained, since mid-20th century [2].

In the absence of strong charge separation and specific intermolecular interactions (like H-bonds), bulk properties of molecular condensed phases, including mp and bp, are

Dedicated in memory of Professor Petr M. Zorky

Y. L. Slovokhotov (✉)
Chemistry Department, Moscow State University, Moscow 119992, Russia
e-mail: slov@phys.chem.msu.ru

A. S. Batsanov · J. A. K. Howard
Department of Chemistry, University of Durham, South Road, Durham DH1 3LE, UK

governed by van der Waals intermolecular forces [3–5]. Most theoretical studies of the structure–property relationships in this class of substances are based on computer simulations and packing analysis (see [5–7] and references therein). A good state-of-art example is a comprehensive theoretical treatment of molecular packing in a set of real and hypothetical crystalline $C_{12}H_{12}$ isomers [8] or in isomers of dichlorobenzene [9].

However, ad hoc packing analysis in organic crystals usually do not give quantitative prediction of their physical constants, because of extreme complexity of the system. At the same time, reported physical data for a huge number of new substances created by synthetic chemistry, have never been analysed in a systematic way. This can be a very promising field of research where new structure-property correlations may be found and, ultimately, explained on physical grounds.

Recently we have found that mp of organic substances reflect the approximate symmetry of their molecular van der Waals surfaces [10], the key factor being a geometry-sensitive short range (''contact'') term of the local van der Waals field that acts on a molecule in a crystal. This additive contact term may be regarded as a perturbation in the average local field created by all molecules. We have suggested that the magnitude of the perturbation depends linearly on the deviation of the molecular van der Waals surface from the idealised *van der Waals group* $\tilde{\mathbf{G}}(\mathbf{U_0})$ which describes the symmetry of the averaged long-range molecular field.

In the present work, we undertook a systematic survey of T_m and T_b data for substituted methanes, ethanes, ethylenes, benzenes, and cyclohexanes, and applied the hypothesis of van der Waals symmetry to the analysis of the observed trends. The experimental T_m and T_b values show a qualitative agreement with this hypothesis, thus pointing to the probable origins of the van der Waals symmetry in crystals and liquids.

Experimental

Mp and bp of organic and inorganic (organometallic) compounds were extracted from the Beilstein [11] and Gmelin [12] databases, respectively, using the CrossFire software [13]. The relevant crystal structures have been retrieved from the Cambridge Structure Database (CSD) and analysed using ConQuest 1.8, Mercury 1.4.1 and Vista programmes [14]. Graphics were prepared using the SigmaPlot software [15].

Results

As an initial step, we have presented T_m and T_b for several series of organic substances as functions of the molecular mass, M. This revealed some remarkable trends, illustrated in the figures below. In the first place, among structurally similar molecules, the corresponding temperatures often show a linear dependence against M^{α}, where $1/2 < \alpha < 1$.

Methane analogues MX_4 and $MX_{4-n}Y_n$

Bp of methane analogues EX_4 (where X = H, alkyl or halogen) correlate linearly with $M^{1/2}$ (Fig. 1). For each series of compounds, the regression line is roughly parallel to that of monoatomic noble gases, but shifted to higher temperatures. There is no drastic difference between molecules with zero and nonzero electric moments, as well as molecules containing X substituents of similar van der Waals dimensions but different masses (e.g., Me and Br) and therefore having different moments of inertia; the corresponding points cluster around the same line. However, bp values of mixed-substituted CMe_nX_{4-n} (X = halogen) with non-zero dipole moment μ and quadrupole moment Q (black triangles in Fig. 1) are elevated by ca. 20–30 K from that of *symm*-EX_4 derivatives. On the other hand, in EEt_4 compounds, bulkier ethyl substituents cause larger increase in bp (by 40–100 K), even though the electric moments of these molecules are much lower than for halides, due to less polar E–C bonds.

The compounds $CR_{4-n}F_n$ with two or more fluorine atoms in a methane-like molecule have much lower bp (Fig. 2a). The depression of bp is also manifested for $EMe_{4-n}Cl_n$ derivatives with $n = 3$ or 4, compared to the less-chlorinated analogues with $n = 1$ or 2 (Fig. 2b). However, one or two polar E–Cl bonds in a molecule bring about an increase of bp, especially for E = Ge and Sn. These two factors cause additional stabilisation of

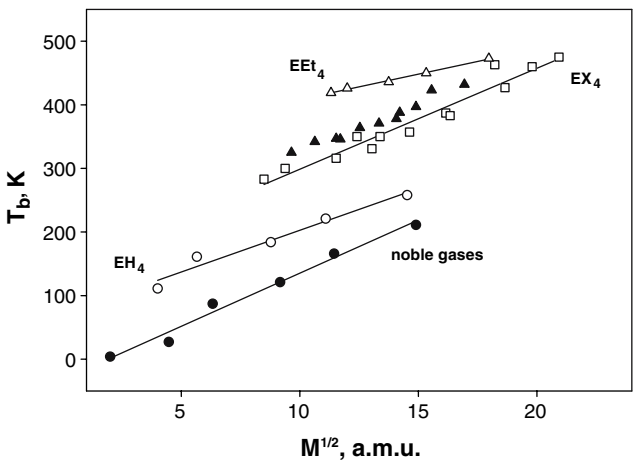

Fig. 1 Boiling points T_b versus the square root of molecular mass $M^{1/2}$ in substituted methane analogues EX_4 (E = C–Pb, X = Me, Cl, Br). Noble gases are shown for reference. Black triangles: mixed-substituted derivatives $CMe_{4-n}X_n$ with nonzero electric molecular moments

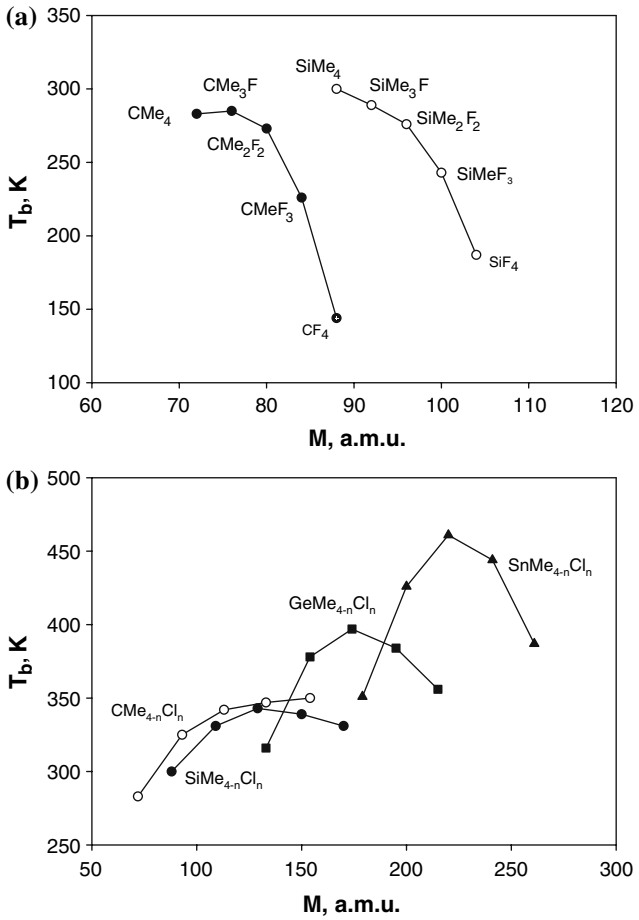

Fig. 2 Electrostatic depression of boiling points in substances composed of tetrahedral molecules with negatively polarised halogen atoms: (**a**) fluorinated derivatives $EMe_{4-n}F_n$ (E = C, Si), (**b**) chlorinated derivatives $EMe_{4-n}Cl_n$ (open circles: E = C, filled circles: E = Si, squares: E = Ge, triangles: E = Sn)

molecular liquids composed of unsymmetrically substituted polar $EMe_{4-n}Cl_n$ molecules, as in the case of E = C (black triangles in Fig. 1). The distinctly nonlinear $T_b(M)$ plot for these compounds cannot be linearised by variation of the exponent in M^{α}. At the same time, bp of tetrafluorides EF_4 increase in the succession CF_4 (144 K) < SiF_4 (187 K) < GeF_4 (237 K), whereas SnF_4 (subliming at 978 K) and PbF_4 (melting at 873 K) are no longer molecular but polymeric solids with hexacoordinated metal atoms [16, 17]. The observed trends of T_b in methane analogues are therefore influenced not only by the molecular van der Waals shape, but also by other factors like electrostatic forces and secondary intermolecular bonding.

Mp of tetrahydrides EH_4 (E = Si to Pb) also increase linearly with $M^{1/2}$ (Fig. 3). This increase is slower than for noble gases; indeed, silane SiH_4 melts 2 K *lower* than methane CH_4. Larger EX_4 molecules display a strongly non-uniform dependence of T_m upon M. In particular, tetramethylsilane $SiMe_4$ (T_m = 171 K) melts 85 K lower

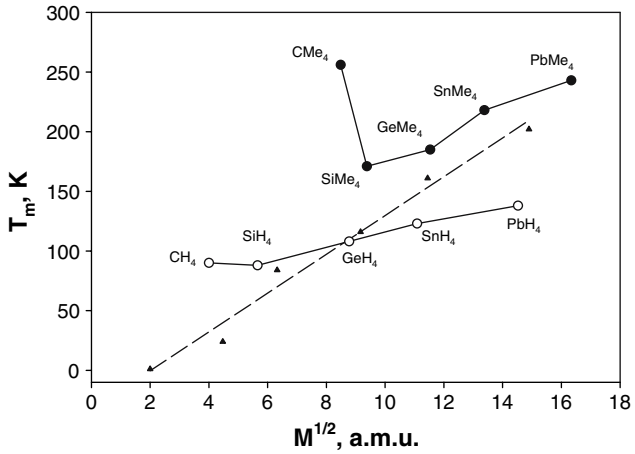

Fig. 3 Melting points T_m in EX_4 derivatives with tetrahedral molecules, as a function of molecular mass. Open circles: EH_4, filled circles: EMe_4. Triangles and dashed regression line: noble gases

than neopentane CMe_4 (256 K), but T_m further increase with the increase of M for the heavier EMe_4 analogues. A similar drop of mp from E = C to E = Si for tetrahaloid EX_4 derivatives is shown in Fig. 4. On the other hand, tetraethyl compounds EEt_4 display a uniform *decrease* of T_m from CEt_4 (240 K) to $PbEt_4$ (143 K).

A remarkable feature in Fig. 4 is a steep increase of T_m from CF_4 to GeF_4 which corresponds the trend in their bp (see above). However, the increase of the number of fluorine substituents in asymmetrically substituted methane analogues progressively destabilises both solid and liquid phases reducing T_m and T_b (*cf.* Fig. 2a and $CMe_{4-n}F_n$ series in Fig. 4).

In the series of chloro-substituted methanes $CH_{4-n}Cl_n$, a monotonic increase of T_b (roughly proportional to $M^{1/2}$) is accompanied by an erratic behaviour of T_m (Fig. 5a). In $CMe_{4-n}Cl_n$ series where the substituents have similar steric dimensions [18], bp and especially mp vary in narrow

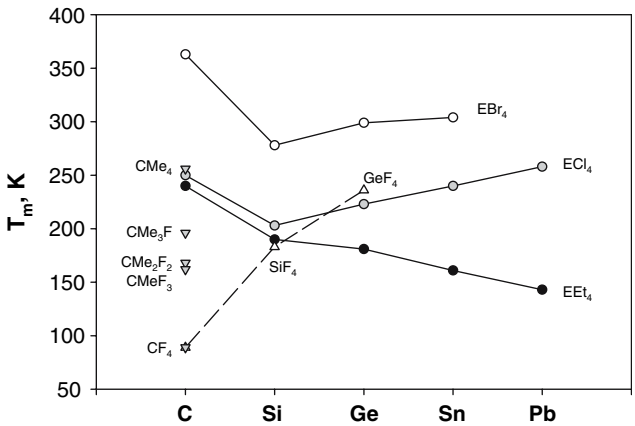

Fig. 4 Melting points of EX_4 derivatives in the C subgroup (scheme). Open circles: X = Br, grey circles: X = Cl, black circles: X = Et. Turned grey triangles: CMe_nF_{4-n} series

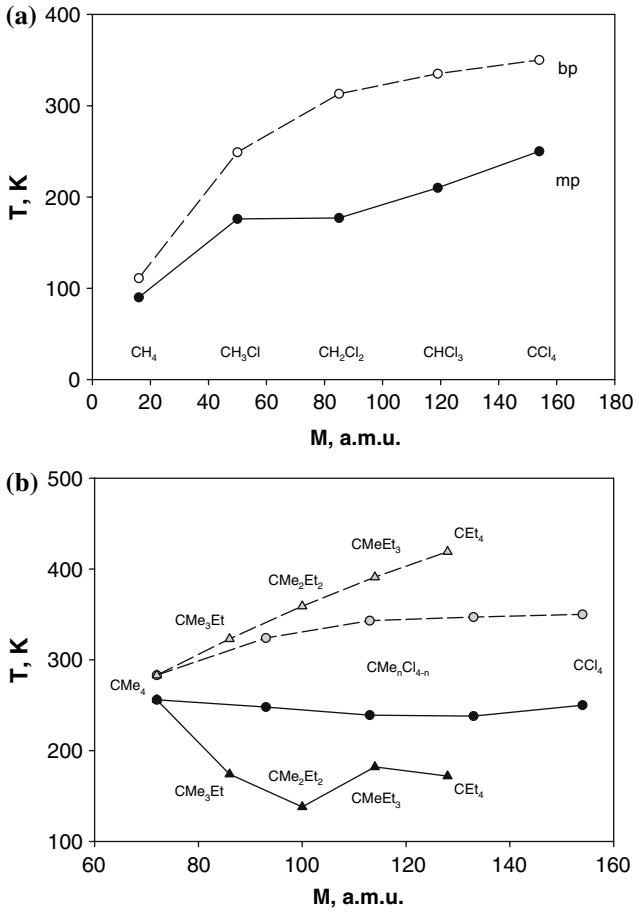

Fig. 5 Plots of mp (solid lines) and bp (dotted lines) versus mass (**a**) in $CH_{4-n}Cl_n$ set, (**b**) in $CMe_{4-n}Cl_n$ (circles) and $CMe_{4-n}Et_n$ sets (triangles)

ranges (283–350 K and 239–256 K, respectively, Fig. 5b). Replacement of one or more of the substituents in *symm*-tetrahedral molecules by heavier and bulkier ones (e.g., Me by Et), often depresses T_m (Fig. 5b). It is noteworthy that T_b and T_m are rather close to each other for CMe_4 (256 and 283 K) but diverge strongly for $SiMe_4$ (171 and 300 K), $GeMe_4$ (185 and 316 K) and other *symm*-tetrasubstituted derivatives with a larger central atom.

Substituted ethanes $C_2H_{6-n}X_n$ and ethylenes $C_2H_{4-n}X_n$

Plots of T_b versus $M^{1/2}$ for substituted ethanes are presented in Fig. 6. The $C_2H_{6-n}Me_n$ series shows a good linear dependence of T_b versus. $M^{1/2}$, with a much steeper increase than in the methane series. The plots for Cl- and Br-substituted ethanes deviate from linearity whereas bp of fluoroethanes *increase* from C_2H_6 to $C_2H_4F_2$ and then *decrease* from $C_2H_4F_2$ to C_2F_6. In pairs of di-, tri- and to tetra-substituted geometrical isomers $C_2H_{6-n}X_n$ (see Scheme 1 for notations), bp differ by up to 51 K (for X = F) in the successions 11- < 12- ($C_2H_4X_2$), 111- < 112- ($C_2H_3X_3$)

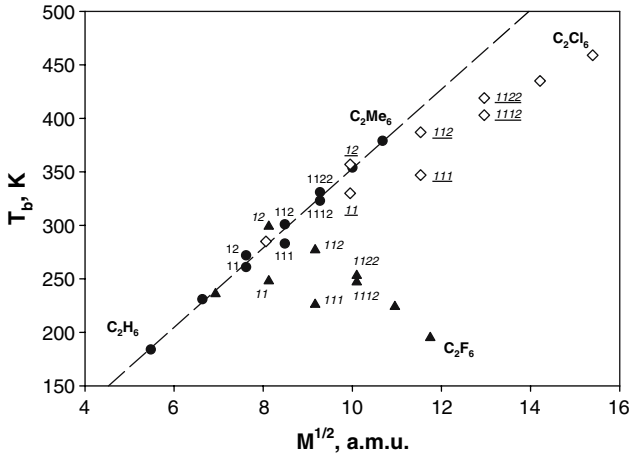

Fig. 6 Boiling point T_b as a function of molecular mass M in substituted ethanes $C_2H_{6-n}X_n$, X = Me (filled circles, plain numbers), $C_2H_{6-n}F_n$ (filled triangles, Italic numbers) and Cl (diamonds, underlined Italic numbers). Isomers are denoted by positions of the substituents at C_2 core (see Scheme 1). Dashes: a regression line for $C_2H_{6-n}Me_n$ series

and 1112- < 1122- ($C_2H_2X_4$; henceforth numbers denote positions of substituents).

Data on silicon analogues Si_2X_6 are more scarce (Table 1). It is noteworthy that whereas ethane $C_2Me_{6-n}Cl_n$ derivatives are subliming solids with $T_m \approx T_b$ at 760 torr, for their $Si_2Me_{6-n}Cl_n$ analogues T_b exceeds T_m by 100–150 K, parallelling the trend mentioned above for the EMe_4 series.

The T_b versus $M^{1/2}$ patterns of substituted ethylenes $C_2Me_{4-n}X_n$ look similar to the patterns of substituted ethanes (Fig. 7). Their main features are almost linear correlation (though with smaller number of points) for X = Me, Cl, Br, a slower growth of bp for Cl- and Br-substituted species as compared to Me-substituted ones and the decrease of bp in fluoroethylenes from $C_2H_2F_2$ to C_2F_4. Differences of bp in three $C_2H_2X_2$ isomers in ''*gem*- < *trans*- < *cis*-'' succession are larger in halogenated species (up to 58 K in $C_2H_2F_2$).

Plots of T_m as functions of M^{α} for substituted ethanes (Fig. 8a) and ethylenes (Fig. 8b) differ substantially from the corresponding $T_b(M^{\alpha})$ patterns; they are not easy to linearise. Among Me_n-substituted ethanes and ethylenes, the lowest T_m is observed for monosubstituted species, i.e., propane $CH_3CH_2CH_3$ and propene $CH_2{=}CHCH_3$. Among isomers mp vary stronger (up to 72 K in $C_2H_2Cl_2$ and 143 K in $C_2H_3Me_3$) and in a succession different from that of bp, e.g., for trisubstituted ethanes (112- < 111-) and disubstituted ethylenes (*gem*- < *cis*- < *trans*-). Note that T_b–T_m difference for these compounds mostly lies in the range of 100–150 K but becomes very small for highly symmetrical C_2X_6 molecules with bulky X substituents (5 K for C_2Me_6 and <1 K for C_2Cl_6 that sublimes at 459 K under 760 torr, see Table 1). Polyfluorinated derivatives, similarly to their

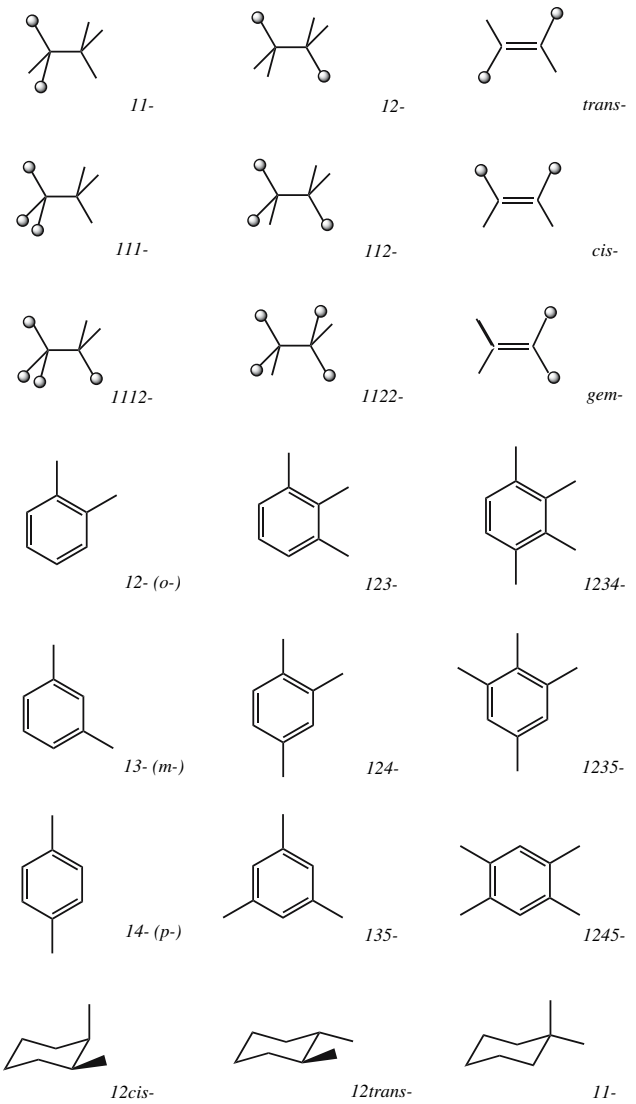

Scheme 1 Notations of isomers

T_b trend, display a strong reduction of T_m, although data are unavailable for some compounds of these series.

Substituted benzenes $C_6H_{6-n}X_n$

T_m and T_b of some substituted benzenes $C_6H_{6-n}X_n$ are listed in Table 2. Bp linearly increase with M ($\alpha = 1$) for

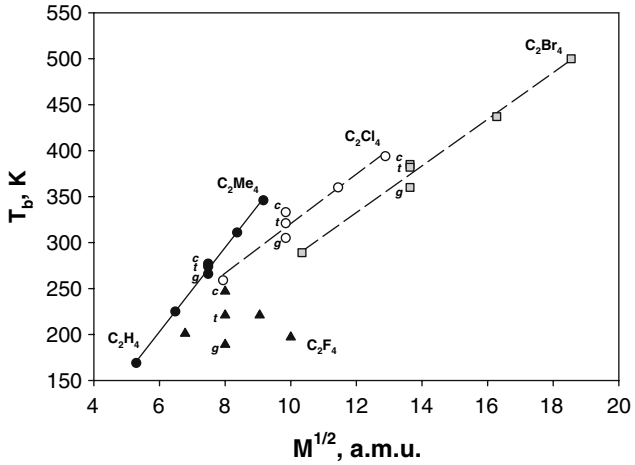

Fig. 7 Boiling points T_b as a function of $M^{1/2}$ in substituted ethylenes $C_2H_{4-n}X_n$, X = Me (black circles), F (black triangles), Cl (open circles), Br (grey squares). $C_2H_2X_2$: *c* = *cis*-, *t* = *trans*-, *g* = *gem*-isomer

X = Me, Cl, Br, but deviate from linearity for extended X substituents (Fig. 9). Similar to ethanes and ethylenes, T_b for Cl- and Br-substituted species increase slower than for Me-substituted analogues.

Three sets of geometrical isomers in the $C_6H_{6-n}X_n$ series display a small variation of T_b (usually within 10 K), generally in the following successions:

$$\begin{aligned} &\text{C6H4X2}: 13- < 14- < 12- \\ &\text{C6H3X3}: 135- < 124- < 123- \\ &\text{C6H2X4}: 1235- < 1245- < 1234- \end{aligned} \quad (1a)$$

Note that melting points in the same sets of isomers can differ by up to 100–150 K and change in different successions [2, 12]:

$$\begin{aligned} &C_6H_4X_2: 13- < 12- < 14- \\ &C_6H_3X_3: 124- < 123- < 135- \\ &C_6H_2X_4: 1235- < 1234- < 1245 \end{aligned} \quad (1b)$$

(see Scheme 1 for notation of isomers). However, mp of trimethylbenzene isomers show an unusual 135- ≈ 124-

Table 1 Melting (T_m) and boiling points (T_b) for high-symmetric ethane-like derivatives $E_2Me_{6-n}Cl_n$ (where E = C, Si)

Compound (*isomers*)		E_2Me_6	E_2Me_5Cl	$E_2Me_4Cl_2$		$E_2Me_3Cl_3$		$E_2Me_2Cl_4$		E_2MeCl_5	E_2Cl_6
				11-	12-	111-	112-	1112-	1122-		
$C_2Me_{6-n}Cl_n$	T_m	374	405	424	433	–[a]	456	449	445	452	459
	T_b	379	405	425	–	–	449	440	–	–	459
$Si_2Me_{6-n}Cl_n$	T_m	286	–	–	285	297	–	288	279	–	274
	T_b	386	407	417	421	422	421	–	426	–	418

[a] Data not available

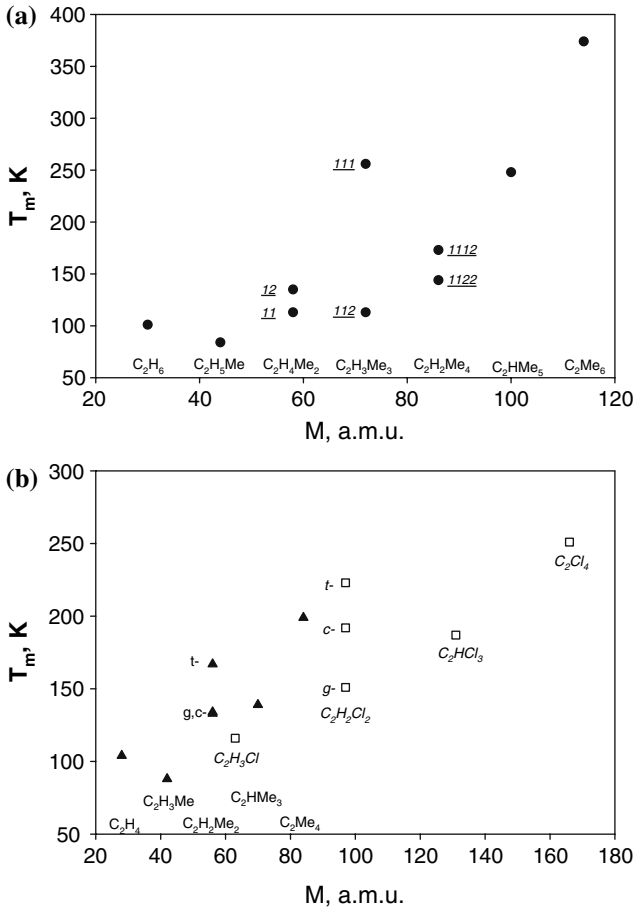

Fig. 8 Melting points T_m as a function of molecular mass M: (**a**) Me-substituted ethanes, (**b**) substituted ethylenes $C_2H_{4-n}X_n$ (filled triangles: X = Me, open squares: X = Cl

< 123- succession. Fluorobenzenes have strongly depressed mp and bp, but the succession of the temperatures for their isomers mostly agree with general trends among substituted species.

Substituted benzene derivatives containing oxygen and/or nitrogen but without strongly H-bonding (e.g., hydroxyl, amino or imino) groups, have elevated mp and bp compared to their hydrocarbon analogues with similar masses and molecular dimensions (Table 2 and Fig. 9b; T_b data for high-boiling species are incomplete due to their decomposition). Thus, mp in $C_6H_{6-n}(OMe)_n$ set lie 40–90 K higher than those of $C_6H_{6-n}Et_n$, whereas bp in OMe-set are elevated by 20–30 K. Melting points in phenols $C_6H_{6-n}(OH)_n$, additionally stabilised by H-bonds, reach 500–540 K. Both T_m and T_b values available for the isomers with neighbouring positions of OH groups (12-, 123- and 1234- in solids; 12- in liquids) are lower due to formation of H-bonded dimers whose hydroxyls cannot participate in a 3D network of H-bonds. Accordingly, their mp successions are altered to 12- < 13- < 14-, 123- < 124- < 135- and 1234- < 1235- < 1245- for n = 2, 3 and 4, respectively.

Substituted cyclohexanes $C_6H_{12-n}X_n$

Substituted cyclohexanes $C_6H_{12-n}X_n$ have more geometric isomers than substituted benzenes $C_6H_{6-n}X_n$, due to a possible axial (*ax*) or equatorial (*e*) orientation of the substituents X relative to the plane of the C_6 ring, as well as *trans*-, *cis*- and *gem*-isomers depending on positions of the substituents relative to each other. The T_b and T_m data available in this family are more limited, mostly covering monosubstituted and some disubstituted species. In Me_n-substituted cyclohexanes, mp is known up to n = 3 and bp up to n = 4 for many isomers.

Monosubstituted cyclohexanes $C_6H_{11}X$ often have lower T_m, but higher T_b as compared with the parent cyclohexane C_6H_{12} (Table 3); the reduction ?T_m of the melting temperature upon substitution is proportional to the van der Waals volume of the substituent X (see [10] for more details). Of the two known undeca-substituted species C_6HX_{11} (where X = F, Cl), the mp of the Cl-derivative is very much lower (by 201 K) than that of C_6Cl_{12}, but C_6HF_{11} melts only 6 K lower than C_6F_{12}. Another available example of undeca-substituted cyclohexane is $C_6HMe_{10}Et$ whose reported mp (458–469 K) is lower than the mp of C_6Me_{12} (568 K).

The available T_b and T_m data for $C_6H_{10}X_2$ (7 isomers, Table 4) and $C_6H_9Me_3$ (12 isomers, Scheme 2) generally resemble the corresponding patterns for substituted benzenes. Thus, T_m of disubstituted isomers with X substituents in different positions of the ring generally follow the ''13- < 12- < 14'' succesion, resembling the mp succesion in $C_6H_4X_2$. Melting points of Me_3-derivatives, except for *gem*-substituted ones, correspond to ''124- < 123'' succesion, and *all-cis*-1,3,5-isomer with the highest (C_{3v}) molecular symmetry has one of the highest T_m (227 K). However, these trends are modified by further geometrical isomers in the cyclohexane family, as can be seen from the compounds in the same series that have the lowest (1,3*cis*, 5*trans*-$C_6H_9Me_3$, C_s symmetry, 166 K) and the highest mp (1,1,2-isomer, C_1 symmetry, 244 K).

Boiling points, known for all Me_3- and most of Me_4-cyclohexanes (Scheme 3), vary considerably among isomers (up to 20–25 K), forming ''13- < 14- < 12-'', ''135- < 124- < 123-'' and ''1234- < 1245- < 1235-'' successions, in similarity with the benzene family. The higher bp values, including those of *cis*-, *trans*- and *gem*-substituted isomers, correspond to non-uniform distributions of Me groups over the ring, either pointing to one side of the average ring plane (e.g., *all-cis* 1234- or 1245-species on Scheme 3) or grouping around the same region of the ring (112- and 1122-isomers). Similarly to hexasubstituted ethylenes C_2X_6 (see above), dodeca-substituted C_6X_{12} species (Table 3) are stabilised as solids and destabilised as liquids. Having a very narrow T_b–T_m gap;

Table 2 Melting (T_m) and boiling points (T_b) of substituted benzenes $C_6H_{6-n}X_n$

Non-associated molecules	T_m, K				T_b, K			
	X = Me	X = F	X = Cl	X = Br	X = Me	X = F	X = Cl	X = Br
1,2-$C_6H_4X_2$	248	239	256	280	417	366	452	498
1,3-$C_6H_4X_2$	225	214	248	266	412	356	446	492
1,4-$C_6H_4X_2$	286	260	327	360	411	361	447	493
1,2,3-$C_6H_3X_3$	248	–[a]	326	360	449	368	492	556
1,2,4-$C_6H_3X_3$	229	238	290	317	442	362	486	548
1,3,5-$C_6H_3X_3$	228	267	336	393	438	350	481	544
1,2,3,4-$C_6H_2X_4$	267	231	319	333	478	368	527	611
1,2,3,5-$C_6H_2X_4$	249	225	325	371	471	357	519	602
1,2,4,5-$C_6H_2X_4$	352	277	413	452	–	362	516	599
Associated molecules	T_m, K				T_b, K			
	X = OH	X = NO_2	X = OMe	X = Et[b]	X = OH	X = NO_2	X = OMe	X = Et[b]
1,2-$C_6H_4X_2$	377	392	296	242	518	592	480	456
1,3-$C_6H_4X_2$	382	363	221	189	553	570	490	454
1,4-$C_6H_4X_2$	444	447	329	230	559	572	485	457
1,2,3-$C_6H_3X_3$	406	398	319	–	573	–	510	–
1,2,4-$C_6H_3X_3$	413	333	293	195	–	–	522	491
1,3,5-$C_6H_3X_3$	492	396	326	207	–	588	529	488
1,2,3,4-$C_6H_2X_4$	433	391	362	285	–	–	–	525
1,2,3,5-$C_6H_2X_4$	439	400	319	252	–	–	544	520
1,2,4,5-$C_6H_2X_4$	505	462	376	242	–	–	–	521

[a] Data not available

[b] Reference data

these compounds sublime easily at ambient pressure with a partial decomposition.

Discussion

Molecular mass as a variable in $T_{m,b}(M^{\alpha})$ plots

It is a common wisdom that among similar molecular substances both T_m and T_b usually increase with increasing molecular mass (M). Even though M does not figure explicitly in any expression of the van der Waals (or, indeed, any other) bonding energy, the reasons for such trend are obvious. The energy of van der Waals attraction is proportional to the number of pairwise atom–atom interactions and hence the number of atoms in the molecule. For substances of similar composition, e.g., hydrocarbons, a roughly linear correlation has been described [7]. On the other hand, the energy of each interaction is proportional to the atomic polarisabilities, which are higher for larger (i.e., usually heavier) atoms.

One can hardly expect a clear-cut mathematical dependence of T_b (or T_m) from M on the basis of the above, purely qualitative considerations, as they relate *via* a number of generalisations which are only approximately true. Nevertheless, in a very simple model of a condensed phase that consists of idealised rigid molecular ''bodies'' (limited by van der Waals atomic spheres), the stabilising van der Waals energy per molecule $-\varepsilon_{vdW}$ is proportional to the accessible area of the molecular surface [7]. The absolute value of energy ε_{vdW} therefore increases when the molecular van der Walls volume increases, giving rise to an approximate power law dependence of ε_{vdW} from a total molecular volume V calculated from atomic increments [3]. Since the steric molecular volume of organic compounds (which usually comprise a very limited selection of elements, viz. C, H, N, O or halogens) is additive on the same crude level of approximation [3, 7], ε_{vdW} may be empirically related to the molecular mass M by a power law

$$\varepsilon_{vdW} \approx KM^{\alpha}, \quad (2)$$

where K is a scaling constant, and α has to be selected between 0.5 and 1 for different sets of organic molecules to achieve better linearisation. It is therefore remarkable that for noble gases, both T_b and T_m are proportional to $M^{1/2}$ (Figs. 1, 3 respectively). For the time being, we accept as a working hypothesis that this correlation represents a general trend for van der Waals condensed phases. Note that

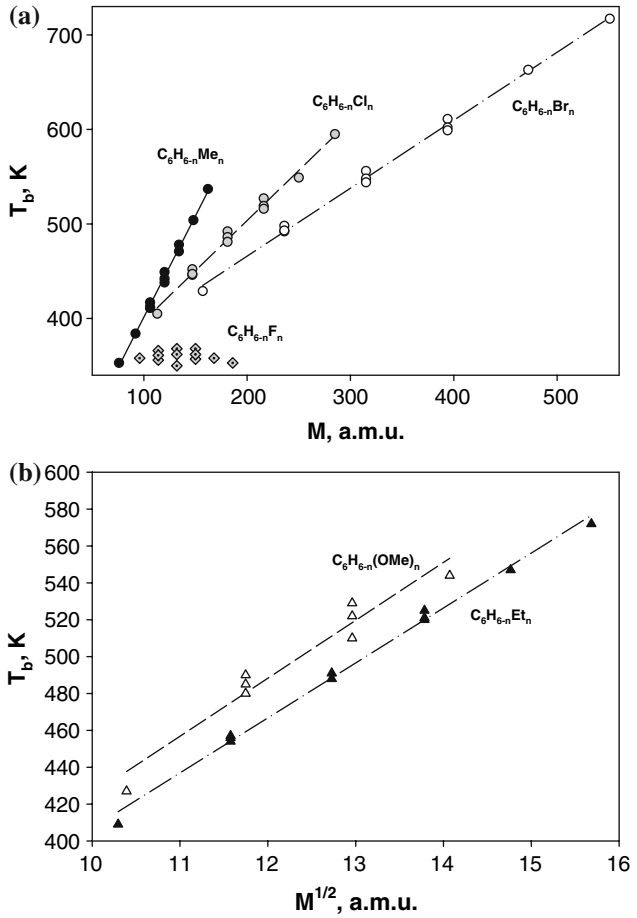

Fig. 9 (**a**) Boiling point T_b as a function of molecular mass M in substituted benzenes $C_6H_{6-n}X_n$ with sphere-like X, (**b**) boiling points T_b versus $M^{1/2}$ for X = Et (filled triangles, dash-dot line) and OMe (open triangles, dashed line); for T_b of isomers see Table 2

all noble gases crystallise similarly in close-packing structures, unperturbed by any steric factors or interatomic interactions other than van der Waals forces.

Melting and boiling temperatures of a substance are the higher, the larger ε_{vdW}. Based on Eq. (2), one may use molecular mass, which is known precisely, instead of van der Waals volume of a molecule (which is a less definite variable) for the analysis of T_m and T_b trends described above. In particular, van der Waals liquids obey Trouton's rule,

Table 4 Melting (T_m, K) and boiling points (T_b, K) of disubstituted cyclohexanes $C_6H_{10}X_2$

Isomers	X = Br, T_m	X = CN, T_m	X = Me, T_m	X = Me, T_b
1,1-	242	337	239	392
1,2-*trans*	268	322	184	397
1,2-*cis*	283	337	223	403
1,3-*trans*	274	323	181	397
1,3-*cis*	385 (193)[a]	311	196	393
1,4-*trans*	385	413	236	393
1,4-*cis*	322	337	183	397

[a] Inconsistent data

$$N_A\ \varepsilon_{vdW} T_b^{-1} \approx 8R \quad (3)$$

(where N_A is Avogadro number, $N_A\varepsilon_{vdW}$ is a latent heat of vaporisation per mole, and R is the universal gas constant) [5]. Thus the T_b of such liquid is linearly related to its molecular cohesive energy ε_{vdW}, hence

$$T_b \approx K' \cdot M^{\alpha} \quad (4)$$

Although no such simple rule is known for T_m, a comparison of T_b versus M^{α} and T_m versus M^{α} plots with the same α may help to reveal differences between melting and boiling trends in a same set of related substances.

General trends in T_m and T_b

Through the analysis of T_b and T_m data in the sets of compounds with closely related molecular structure one can find the main factors that define stability of the corresponding condensed phases. In particular, mp and bp of *symm*-tetrasubstituted methanes CX_4 are determined mostly by van der Waals forces since their molecules of T_d symmetry have zero dipole moment (μ=0), zero quadrupole moment (Q = 0), and a scalar moment of inertia I. Mixed derivatives $CR_{4-n}X_n$ (where R = H, Me, and X = halogen) have nonzero molecular electric moments that notably influences on their properties (see Fig. 1). On the other hand, methane and some other *symm*-substituted CX_4,

Table 3 Melting (T_m) and boiling points (T_b) of mono-, undeca- and dodecasubstituted cyclohexanes

Compound	T_m, K					T_b, K				
	X = H	X = Me	X = F	X = Cl	X = Br	X = H	X = Me	X = F	X = Cl	X = Br
$C_6H_{11}X$	*280*	147	285	230	216	*356*	374	373	415	437
C_6HX_{11}	*280*	–[a]	320	358	–	*356*	–	336	–	–
C_6X_{12}	*280*	568	326	559	–	*356*	–	326	–	–

[a] Not available

Reference data for C_6H_{12} are shown in Italic

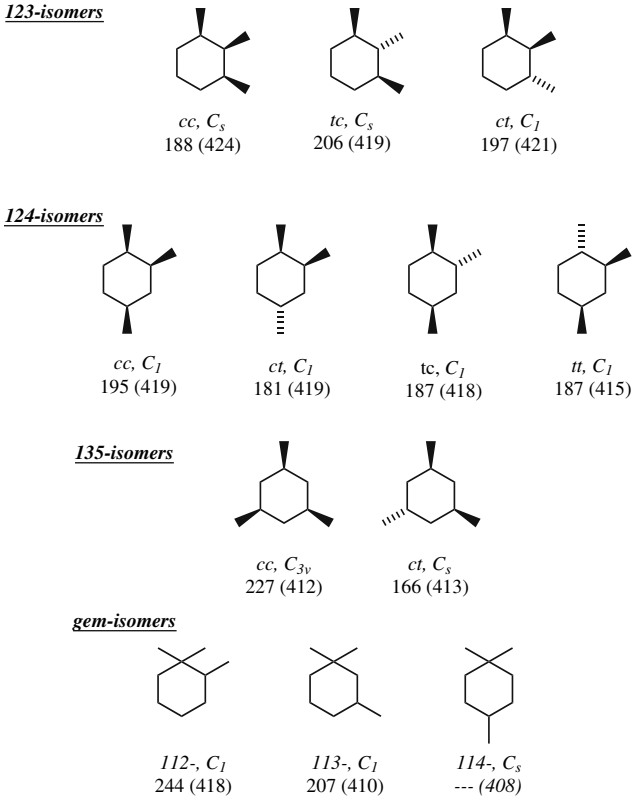

Scheme 2 Point groups, melting temperature, and boiling temperature (in brackets) of trimethylcyclohexane isomers (*c* = *cis*-, *t* = *trans*-)

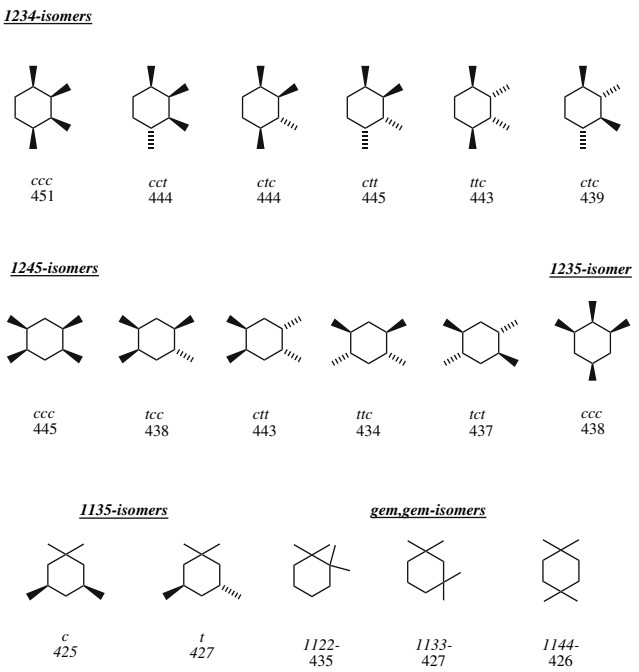

Scheme 3 Notations and boiling points for known isomers of tetramethylcyclohexanes

C_2X_6 and C_6X_{12} compounds have a roughly spherical molecular van der Waals shape whereas extended X substituents (e.g., CN or Et) make this shape less symmetrical. Deviations of asymmetric methane analogues from a simple linearised dependence of T_b (Fig. 1) and T_m (Fig. 3), shown in Figs. 2, 4, 5 are therefore due to a balance of electrostatic forces, molecular van der Waals asymmetry and specific bonding (see below).

The corresponding $T(M^\alpha)$ plots in Figs. 1–9 reveal the following general trends:

I. Boiling point T_b increases smoothly and regularly with M; a difference of T_b among isomers is usually small (10–20 K)
II. Melting point T_m depends non-uniformly on M with a stronger difference of T_m among isomers (*ca.* 50–100 K)
III. In the same set of isomers different successions of T_m and T_b are observed.

Note that bulkier substituents usually bring higher T_b, but very often depress T_m in a set of closely related substances. For example, mp decreases strongly from benzene (279 K) to toluene (178 K) and from cyclohexane (280 K) to methylcyclohexane (146 K), whereas the bp of the same monosubstituted derivatives increases uniformly as a steric volume (and mass) of the molecule increases: C_6H_6 (353 K) $\rightarrow$ C_6H_5Me (384 K) and C_6H_{12} (356 K) $\rightarrow$ $C_6H_{11}Me$ (374 K).

Relative T_m and T_b values in all sets of isomers considered above are summarised in Table 5. Physical causes of the known dependence of T_m of organic compounds on molecular geometry [2, 3, 5] have been analysed from the symmetry viewpoint in our previous communication [10]. Variations of T_b at 760 torr between isomers, discussed here, are less common. Most intriguing are the *different* successions of T_b and T_m in the same sets of isomers (see Table 5)—a fact that has to be explained theoretically.

Hypothesis of van der Waals symmetry

A relationship between bulk characteristics of substances and their molecular shape, is based on the long-known fundamental property of a molecule to occupy a finite volume in three-dimensional space. Considering molecules as bodies (rather then sets of point masses and charges), densely packed ''bump-to-hollow'' in a molecular crystal, was a key postulate proposed by Kitaigorodskii as the cornerstone of organic crystallography [3]. With this idea in mind we can attempt to explain the T_m and T_b trends, by comparing the symmetry of the local field created by all molecules in a condensed phase, with the symmetry of molecular van der Waals ''bodies''.

Table 5 Melting point (T_m) and boiling point (T_b) orders among isomers of some organic compounds (Beilstein database [11]; for notation of the isomers see Scheme 1)

	T_m	T_b
Ethanes $C_2H_{6-n}X_n$ (n = 2–4)	11- < 12-	11- < 12-
	112- < 111-[a]	111- < 112-
	–[b]	1112- < 1122-
Ethylenes $C_2H_2X_2$	*gem*- < *cis*- < *trans*-	*gem*- < *trans*- < *cis*-
Benzenes	13- < 12- < 14- (*m*- < *o*- < *p*-)	13- < 14- < 12- (*m*- < *p*- < *o*-)
$C_6H_{6-n}X_n$, n = 2–4	124- < 123- < 135-	135- < 124- < 123-
	1235- < 1234- < 1245-	1235- < 1245- < 1234
Cyclohexanes	13- < 12- < 14*tr*- ≈ 11	13- ≈ 14- < 12-
$C_6H_{12-n}X_n$, n = 2, 3	13*cis*5*tr* < 124- < 123- < 13*cis*5*cis* < 112-	135- < 124- < 123-

[a] 112- > 111- for X = F

[b] No definite succession observed

Crystals with close packing of molecules display a narrow range of such bulk characteristics as a packing coefficient (0.65–0.80), van der Waals energy per atom (5–10 kJ/mole) and molecular coordination number (10–14) [3, 5, 7]. On a very qualitative level, dense molecular packing in such crystals may be deduced from the close packing of identical van der Waals spheres (e.g., in solid noble gases), whereas different van der Waals radii of the atoms and their tightening into molecules by interatomic bonds may be considered as a perturbations of packing (Fig. 10). A measure of such perturbation is a ''contact'' term in the local van der Waals field that acts on each molecule in a crystal. This assumption was actually a basis of our hypothesis of van der Waals symmetry [10].

A qualitative comparison of molecular shapes has been suggested two decades ago by Kitaigorodskii in his theoretical analysis of solid solutions of organic compounds [19]. To construct a more quantitative model, we have postulated in [10] that the local van der Waals field U that acts on a middle-sized molecule (of several dozen atoms) in a condensed phase, may be presented as

$$U = U_0 + W, \tag{5}$$

where U_0 is a van der Waals potential arising from all *distant* molecules (and possibly from outer fragments of the nearest ones), and W is a short range (''contact'') term originating from the molecule's immediate environment (Fig. 11). We suppose that the averaged U_0 term, randomised by the influence of many molecules and fragments at distances larger than a close non-valence contact, is not sensitive to the molecular geometry whereas the perturbation term W is geometry sensitive.

As shown schematically in Fig. 11, the topology of W reflects the shape of the molecule composed additively of rigid van der Waals atomic spheres. On the other hand, spatial properties of the U_0 term are determined by the average structure of a condensed phase. The latter is different for molecular crystals and molecular liquids due to vacancies and ''jumping'' of molecules in a liquid state [4]. Trends in the structure-dependent bulk properties, like mp and bp, in a series of closely related compounds therefore reflect the similarity—or dissimilarity—between W and U_0, i.e., how well the molecular ''bodies'' fit to the averaged local potential U_0 in a given condensed phase.

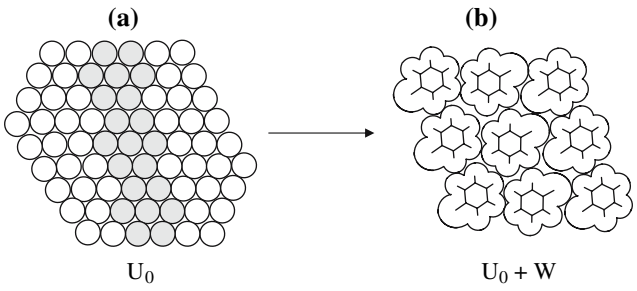

Fig. 10 Transformation of a close packing of van der Waals spheres (**a**) into a close packing of molecules (**b**) as a result of perturbation (schematic)

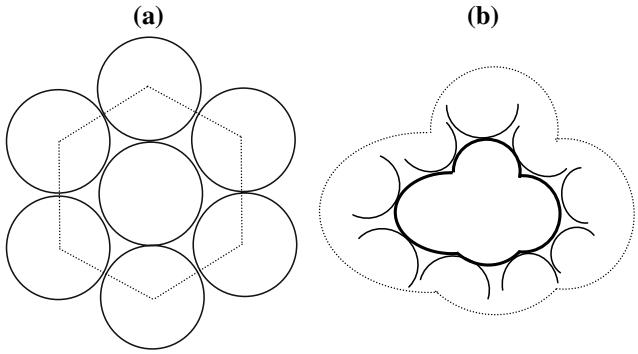

Fig. 11 Origin of the contact term W in (**a**) a dense packing of van der Waals spheres, (**b**) a close packing of low-symmetry molecules (schematic)

One can reasonably believe that spatial properties of U_0 are the same in a set of isomers of the same condensed state (i.e., all solid or all liquid). We also postulate that the W term, determined mostly by the shape of a molecule, remains unchanged upon melting if vacancies are randomly distributed over the average local molecular environment in a liquid [4, 5]. The model thus links a different succession in physical properties of isomers, or of other closely related substances, in crystal and liquid phases to variations of their U_0 term in Eq. (5).

To quantify deviations in van der Waals shape of different molecules from the main local field, a reference idealised point group, called *van der Waals group* $\tilde{\mathbf{G}}(\mathbf{U_0})$, has been suggested [10]. Such a group corresponds to the approximate symmetry of the main term U_0 in Eq. (5). The perturbation introduced by W is proportional to the index of molecular asymmetry $\boldsymbol{a}_s$, a measure of the gap between the molecule's shape and the symmetry of the U_0 field as expressed by the van der Waals group $\tilde{\mathbf{G}}(\mathbf{U_0})$:

$$a_s = (1\backslash V)\sum_i \Delta V(\tilde{g}_i). \qquad (6)$$

Here $\Delta V(\tilde{g}_i)$ is a difference in van der Waals volume between a molecule and its image after transformation by the symmetry element $\tilde{\mathbf{g}}_i \in \tilde{\mathbf{G}}$, V is the van der Waals volume of the molecule, and the sum is taken over all elements of $\tilde{\mathbf{G}}$.

Molecular asymmetries in the main crystal field, calculated in [10] for several classes of organic compounds, displayed a good correlation with their melting points. In methane analogues EX_4 (see Figs. 3–5), not considered in [10], van der Waals asymmetry increases with the increase of the E–X bond length, making larger tetrahedral molecules ''less spherical''. A general decrease of T_m from CEt_4 to $PbEt_4$, where a central atom is protected from additional bonding by the bulky ethyl substituents (Fig. 4), is therefore due to an increase of steric perturbation W in this row. The decrease of T_m for bulkier molecules is also observed in $CMe_{4-n}Et_n$ set (Fig. 5b). The non-uniform T_m versus $M^{1/2}$ patterns in other EX_4 substances shown in Figs. 3 and 4, is due to destabilisation of the crystal packing by increased van der Waals asymmetry from C to Si and further stabilisation by secondary bonding which grows from Si to Pb.

Van der Waals symmetry in crystals and liquids

The idealised symmetry of the main crystal field U_0 may be taken, in the crudest approximation, as the O symmetry of van der Waals field in the face centered cubic (fcc) close packing, which is the actual atomic packing in crystalline noble gases [20] (see Figs. 10, 11). In fact, such approximation is not as far-fetched as it seems, if one takes into account that (i) *all* known atomic van der Waals radii vary only by a factor of 2, and if we exclude hydrogen and iodine, only by 30%; (ii) packing coefficients in molecular crystals do not differ from the ideal close-packing value of 0.74 by more than 8–12%. From this viewpoint, molecular asymmetry corresponding to formula (6) in a crystalline phase is the sum of deviations of the molecule's van der Waals shape from the O_h group. Difference between T_b and T_m trends among isomers therefore corresponds to the molecular liquid being described by a different $\tilde{\mathbf{G}}(\mathbf{U_0})$group than the molecular crystal, providing different qualitative successions of the molecular $\boldsymbol{a}_s$ values in these two condensed phases.

The most prominent differences in mp and bp trends in Table 5, is a relative decrease of T_b for highly symmetric derivatives that have high T_m, e.g., *trans*-disubstituted ethylenes $C_2H_2X_2$, 1,1,1-trisubstituted ethanes $C_2H_3X_3$, 1,4-benzenes, *trans*-1,4-cyclohexanes, etc. Their high-boiling isomers (*cis*-$C_2H_2X_2$, 1,2-benzenes, etc.) have lower molecular symmetry. This effect is stronger for 1,1,1-$C_2H_3X_3$ and 1,3,5-$C_6H_3X_3$ species possessing the highest molecular symmetry (C_{3v} and D_{3h}, respectively). These particular isomers usually have the highest T_m and lowest T_b in the corresponding sets. At the same time, such isomers as *gem*-$C_2H_2X_2$ or 1,2,3,5-$C_6H_2X_4$, having large van der Waals asymmetry in the crystal phase, are both low-melting and low-boiling. Different mp and bp values in pairs of isomers whose molecules have the same point symmetry, but different van der Waals shape (*gem*- and *cis*-$C_2H_2X_2$, 1,2- and 1,3-$C_6H_4X_2$, etc.) therefore reveal some systematic differences in their W term, both in solid and liquid phases.

The bp are generally higher for isomers with a smooth anisotropic van der Waals surface, viz. 1,2,3-$C_6H_3X_3$, 1,2,3,4-$C_6H_2X_4$ and their *all-cis*-analogues in cyclohexane family. Most probably, this reflects a particular topology of the local field U in a liquid phase.

The existence of vacancies in a liquid phase [5] violates the dense packing and induces anisotropy in the local $U_0^{(L)}$ term. The corresponding change of van der Waals group $\tilde{\mathbf{G}}(\mathbf{U_0})$ will transform the W term of highly symmetric molecules from a weak perturbation in a solid to a strong perturbation in a liquid. For example, a removal of one vertex from the cuboctahedron (the closest environment of a sphere in the fcc packing) reduces the local symmetry of the environment from O_h to C_{2v} and the coordination number from 12 to 11, whereas two vacancies in a cubo-octahedral environment correspond to four ''isomeric'' arrangements with $N = 10$ (Fig. 12). A corresponding decrease in N by 16–17 % agrees well with the experimentally observed drop of density of organic compounds upon melting [5].

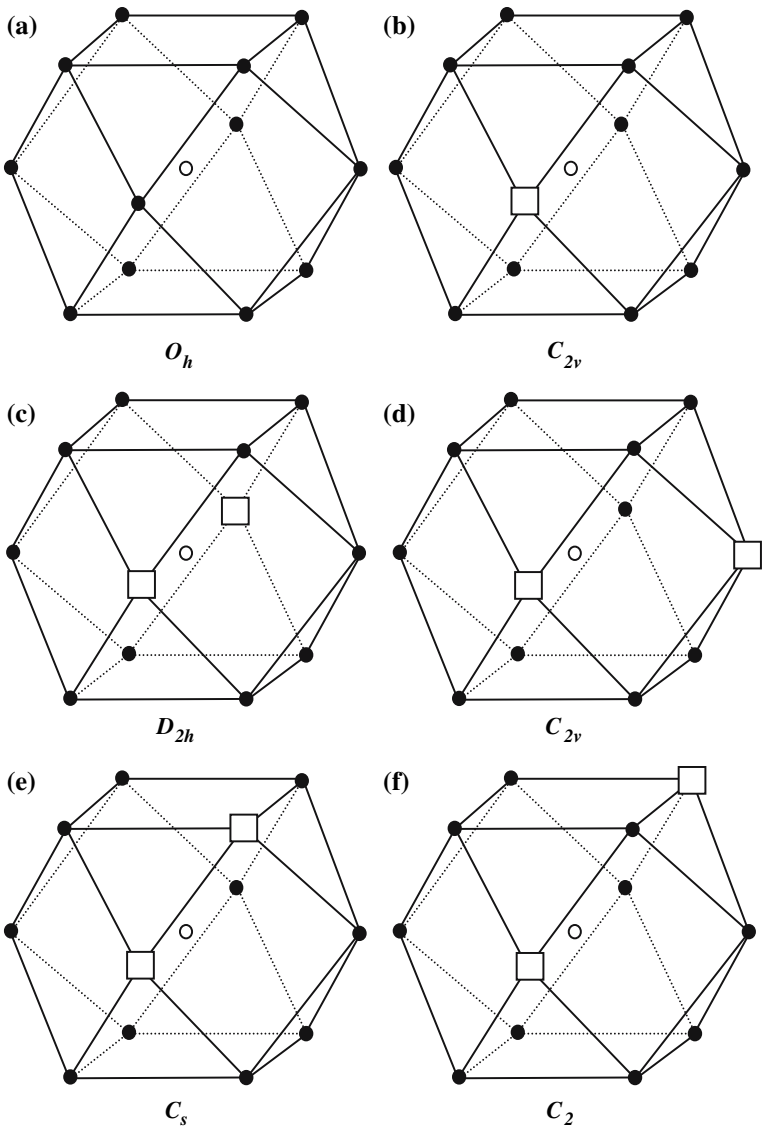

Fig. 12 Idealised closest molecular environment and their model van der Waals groups: (**a**) regular cubooctahedron, (**b**) a cubooctahedron without one vertex, (**c**)–(**f**) four ''isomers'' of a cubooctahedron without two vertices. The symbol '□' denotes a vacant site

For a rigid local environment, molecular asymmetry in a model ''liquid'' becomes a weighted sum over all possible arrangements of vacancies [e.g., (b)–(f) in Fig. 12]:

$$<a_s> \; = \; \Sigma w_i a_s^{(i)}, \qquad (7)$$

where $\boldsymbol{a}_s^{(i)}$ is the asymmetry index of a molecule in the *i*th environment, and the weight w_i is its relative population. Thus, w_i values for the polyhedra in Fig. 12 c–f should relate as 1:2:4:4 on simple geometric considerations. Likewise, a possible redistribution of 10 or 11 surrounding molecules in a liquid, will still correspond to the symmetry lower than cubic.

The neighbouring positions of vacancies in two of the distorted 10-vertex polyhedra [(d) and (e) in Fig. 12] qualitatively corresponds to a non-uniform distribution of substituents around the ring in high-boiling isomers of substituted benzenes and cyclohexanes. On the other hand, highly symmetrical molecules must have a smaller deviation from the cubic closest environment (Fig. 12a) but a larger misfit to any lower-symmetry van der Waals field. As a result, compounds built of such molecules will have high T_m but low T_b, in a qualitative agreement with the experimental observations.

The ''gauge'' in the symmetry of the van der Waals term U_0 in crystals and liquids helps to explain the observed high mp and low bp of substances composed of molecules with a rounded van der Waals shape—e.g., neopentane CMe_4 that has the highest melting point (256 K) and the lowest boiling point (283 K) in the whole family of C_5 hydrocarbons (see [10]). The same is true for the compounds with most symmetric sphere-like molecules (adamantane, C_2Me_6, C_6F_{12} etc.) that sublime easily at 760 torr [2]. The shape of these molecules causes a weak

perturbation of the average van der Waals field $U_0^{(C)}$ in a crystal but a strong perturbation of $U_0^{(L)}$. So the liquid phase does not exist at the temperature where thermal motion destroys the crystal state, and the substance passes directly into gaseous state.

Non-van der Waals factors influencing T_m and T_b

Differences of van der Waals field in organic compounds have to be compared with other factors that also may be in theory responsible for the observed trends of T_m and T_b. These factors are (i) Coloumb intermolecular interactions, (ii) secondary intermolecular bonding and (iii) geometry-sensitive entropy changes $T\Delta S$ in melting and boiling of the organic substances.

Electrostatic forces

Coloumb intermolecular interactions caused by polar bonds in the molecules may modify T_m and T_b in two opposite ways. Firstly, a strong $X^{\delta-}\cdots X^{\delta-}$ intermolecular electrostatic repulsion between substituents bearing partial negative charges (e.g., X = F or Cl) reduce both T_b and T_m (Figs. 2, 4, 6b, 9a). The destabilising effect of close intermolecular F···F contacts have been deduced earlier from packing analysis of F-substituted organic compounds [21]. A less steep slope of T_b versus M^{α} plot for Cl- and Br-substituted derivatives in comparison with Me-substituted ones (Figs. 6, 7, 9a) may also be due to a destabilising X···X repulsion of (more weakly) charged halogen atoms. Secondly, positively charged H atoms bonded to electronegative X (OH, NH_2, SH groups, etc.) give rise to a stabilising $X^{\delta-}$–$H^{\delta+}\cdots X^{\delta-}$ hydrogen bonding [5, 22]. A weaker electrostatic attraction may be responsible for other types of secondary interactions like $NO_2\cdots NO_2$ interactions in nitro-substituted organic compounds. Therefore, electronegative substituents not containing H atoms (OR, SR, COOR, NR_2, CN, etc., where R is a hydrocarbon moiety) elevate T_m and T_b in comparison with the related non-polar substances (Figs. 1, 9b).

Secondary bonding

Apart from H-bonds, other sorts of a weak attraction may exist between adjacent molecules having atoms with low coordination numbers (S···O=C, Hg···X, Au···Au, $I_2\cdots I^-$, etc.) [6, 23]. A special case of ''additional'' ligands weakly bonded to a non-saturated coordination centre is well known in inorganic chemistry. These secondary bonding interactions elevate both T_m and T_b. Higher mp and bp of tetrafluorides in the CF_4–GeF_4 series, where polarity of E–F bonds increases (see Figs. 2, 4), is most probably due to such additional intermolecular E···F bonding to larger central atoms. A survey of the CSD reveals that Ge and Sn atoms are usually penta- or hexacoordinated in the solid state (Fig. 13). A weak additional secondary bonding of Si is typical for tetracoordinated silicon derivatives [26] (where it is probably more than compensated by a strong van der Waals asymmetry, see Figs. 3, 4). The increase of the melting temperature in EX_4 series with relatively small X substitutents, like halogens, from E = Si to E = Pb, may also be due to the secondary E···X intermolecular coordination.

It is noteworthy that both stabilising (NO_2, CN) and destabilising (F) substituents usually do not alter a general order of T_m and T_b among isomers (except where strong H-bonds exist, e.g., in *ortho*-dihydroxo derivatives, discussed in *RESULTS*). In most cases, bp and mp of all isomers are uniformly shifted to higher or to lower temperatures by electrostatic interactions and/or secondary bonding. Moreover, similar T_m (T_b) trends are observed for the compounds with opposite polarity of substituents (e.g.,

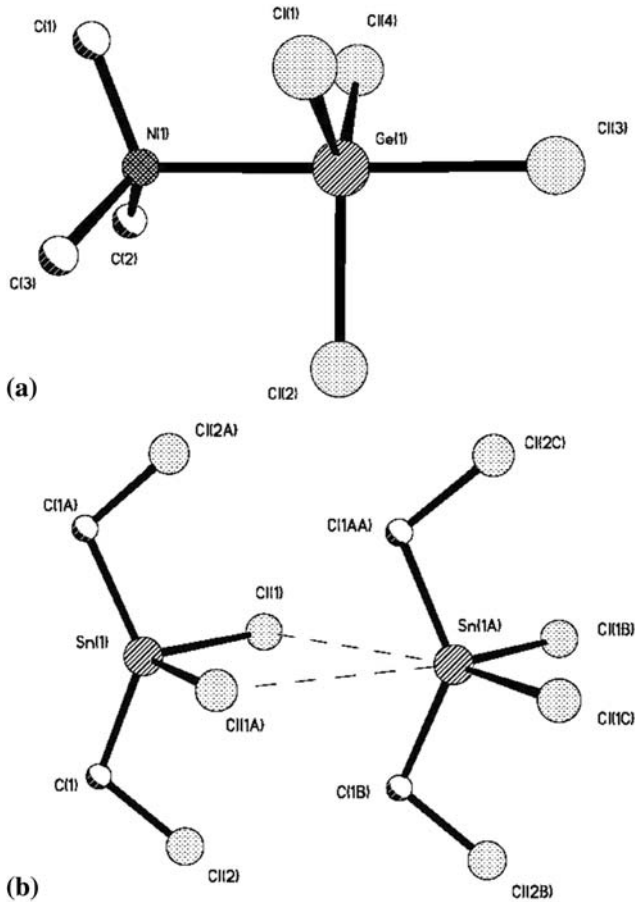

Fig. 13 Two examples of secondary bonding with a formally four-coordinated central atom of group 14 elements: (**a**) $GeCl_4{\cdot}NMe_3$ [24], (**b**) $Sn(CH_2Cl)_2Cl_2$ [25]. Atomic coordinates have been taken from CSD

Me- and F-substituted isomers) as well as with different types of chemical bonding (benzene vs. cyclohexane derivatives). Therefore, both electrostatic and specific intermolecular interactions cannot be a primary reason for the observed regular geometry-dependence of mp and bp, although they may alter a general succession in some particular cases. Note that mp and bp variations are smaller (and in the case of bp may be negligible) for isomers containing X and Y substituents with opposite polarity but similar steric dimensions (e.g., Me and Cl). This fact strongly supports the principal role of van der Waals forces, in their molecular field, for all non-ionic organic substances.

Geometry-dependent $T\Delta S$ term

The discussion of T_m and T_b purely in terms of energy is valid only if discrete changes of entropy ΔS in the phase transitions are not very sensitive to the molecular geometry. It has been noticed [8] that for real and hypothetical polymorphs of several $C_{12}H_{12}$ isomers, the computed $T\Delta S$ terms are comparable with ΔH. However, a measurable difference in entropy of melting or boiling between different isomers with rather similar, compact and mostly rigid molecules discussed here, may be ruled out. This is indirectly supported by the lack of noticeable dependence of either mp or bp from the molecular moments of inertia. (Note that most I_{jj} values, e.g., in disubstitutes benzenes $C_6H_4X_2$, uniformly increase in the 12- < 13- < 14- succession, in disagreement with both T_m and T_b trends).

The latent heat ΔH of melting or vaporisation at the corresponding temperature evidently is

$$\Delta H = T\Delta S, \tag{8}$$

since the change of Gibbs potential $\Delta G = \Delta H - T\Delta S$ between two phases is zero at the point of equilibrium. A strict account for changes of entropy upon melting and boiling requires calculating statistical sums for organic substances in the liquid phase [4]. Since there is no accepted model of the liquid state to make such calculations straightforward, we compare here measured thermodynamic parameters [27] for several substituted benzenes with their T_m and T_b (Table 6). No direct correlation of T_m with either ΔH or ΔS at the melting temperature can be observed in various monosubstituted benzenes, as well as in the ''anomalous'' set of trimethylbenzenes (see above), whereas for $C_6H_4X_2$ isomers (X = Me, Cl) ΔH_m and T_m are of the same order. In a good agreement with the Trouton's rule [Eq. (3)], the ΔS values at boiling temperatures are almost constant (Table 6). Standard enthalpy of evaporation at 298 K, shown in the neighbouring column, therefore displays a good linear correlation with T_b (Fig. 14). Thus changes of entropy in Table 6 are not very sensitive to the molecular structure. We are therefore left with ''static'' van der Waals interactions, as the most probable reason for

Table 6 Melting (T_m) and boiling (T_b) temperatures, enthalpy (ΔH_m) and entropy (ΔS_m) of melting, standard enthalpy of vaporisation at 298 K ($\Delta H_{vap}{}^0$) and entropy of vaporisation at T_b (ΔS_b) in benzene family (data taken from [27])

	T_m, K	T_b, K	ΔH_m, kJ/mol	ΔS_m, J/(mol K)	$\Delta H_{vap}{}^0$, kJ/mol	ΔS_b, J/(mol K)
C_6H_6	279	353	9.9	35.5	33.9	87.0
C_6H_5Me	178	384	6.6	37.2	38.0	86.5
C_6H_5F	231	358	11.3	47.0	34.6	87.2
C_6H_5Cl	228	405	9.6	41.9	41.0	86.9
C_6H_5Br	242	428	10.7	44.0	44.5	–[a]
C_6H_5I	242	461	9.8	40.3	47.7	–
$C_6H_5CF_3$	244	375	13.8	56.5	37.6	86.9
1,2-$C_6H_4Me_2$	248	417	13.6	54.9	43.5	86.8
1,3-$C_6H_4Me_2$	225	412	11.6	51.4	42.7	86.7
1,4-$C_6H_4Me_2$	286	411	17.1	59.7	40.0	86.9
1,2,3-$C_6H_3Me_3$	248	449	8.2	33.0	49.1	–
1,2,4-$C_6H_3Me_3$	229	442	12.6	56.0	47.9	–
1,3,5-$C_6H_3Me_3$	228	438	9.5	41.7	47.5	–
1,2-$C_6H_4Cl_2$	256	452	12.9	–	50.5	–
1,3-$C_6H_4Cl_2$	248	446	12.6	–	50.6	–
1,4-$C_6H_4Cl_2$	327	447	18.1	–	55.5	–

[a] Data not available

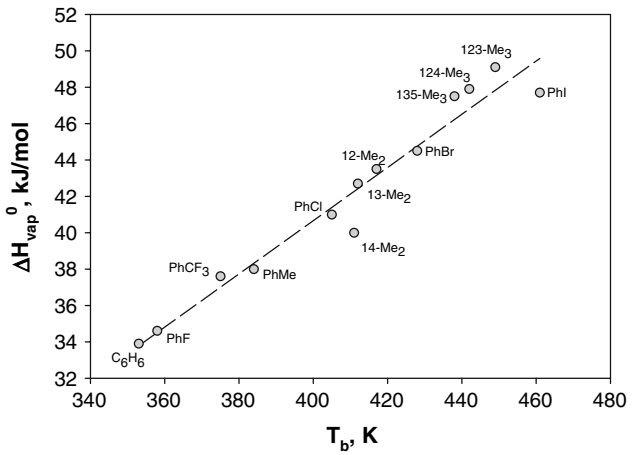

Fig. 14 Linear correlation of standard enthalpy of vaporisation at 298 K $\Delta H_{vap}{}^{0}$ with boiling point T_b in substituted benzenes [27]

the variations of T_m and T_b in the sets of closely related compounds.

Conclusions

The available melting and boiling temperatures of organic compounds and related substances strongly depend upon van der Waals volume and shape of their molecules. The relationship of T_m with a molecular structure is known for a long time in physical organic chemistry whereas T_b shows different dependence upon molecular geometry. Both T_m and T_b trends may be explained on the basis of a model that represents a total van der Waals field U in a condensed phase, as a sum of the averaged long-range local field U_0 and a short-range ''contact'' term W determined by a molecular geometry. A symmetry of crystal's $U_0{}^{(C)}$ and liquid's $U_0{}^{(L)}$ local field is different due to vacancies in the nearest molecular environment in a liquid phase. Perturbations of U_0 by W are supposed to correlate with a discrepancy between the symmetry of the molecular steric shape and the symmetry of the van der Waals group $\tilde{\mathbf{G}}(\mathbf{U_0})$ of the U_0 term in a given condensed phase. Variations of such a misfit among isomers explain qualitatively the different successions of their T_m and T_b, including lower boiling temperatures of liquids composed of high-symmetric molecules. A more rigorous theoretical treatment, including model calculations of both U_0 and W terms, is required for a quantitative analysis of T_m and T_b data.

Acknowledgement Y.L.S is grateful to the Royal Society of London and the Russian Foundation for Basic Research (grant 06–03–08192) for a financial support. J.A.K.H. thanks the EPSRC for a Senior Research Fellowship.

References

1. Silverman RB (2004) The organic chemistry of drug design and drug action, 2nd edn. Academic Press, San Diego
2. Herbrandson HF, Nachod FC (1955) In: Braude EA, Nachod FC (eds) Determination of organic structures by physical methods. Academic Press, New York, p 3, and references therein
3. Kitaigorodskii AI (1973) Molecular crystals and molecules. Academic Press, New York
4. Gray CE, Gibbins KE (1984) Theory of molecular fluids, vol 1. Clarendon, Oxford
5. Israelachvili J (1991) Intermolecular & surface forces, 2nd edn. Academic Press, New York
6. Desiraju GR (1989) Crystal engineering: the desing of organic solids. Elsevier, Amsterdam
7. Gavezotti A (1994) In: Bürgi H.-B, Dunitz JD (eds) Structure correlation, vol 2. WCH, Weinheim, p 509
8. Dunitz JD, Filippini G, Gavezzotti A (2000) Helv Chim Acta 83:2317
9. Boeze R et al (2001) Helv Chim Acta 84:1561
10. Slovokhotov YuL, Neretin IS, Howard JAK (2004) New J Chem 28:967
11. Beilstein Institut zur Förderung der Chemischen Wissenschaften licenced to Beilstein Chemie Daten und Software GmbH and MDL Information Systems GmbH, Version 4, December (2002)
12. 2002 Gesellschaft Deutscher Chemiker licensed to MDL Information Systems GmbH, Version 4, December (2002)
13. http://www.mimas.ac.uk/crossfire/docs.html
14. Allen FH, Taylor R (2004) Chem Soc Rev 33:463
15. http://www.systat.com/products/SigmaPlot
16. Hoppe R, Daehne W (1962) Naturwissenschaften 49:254
17. Hoffmann R, Hoppe RZ (1969) Anorg Allg Chem 368:271
18. Emsley J (1989) The elements. Clarendon, Oxford
19. Kitaigorodskii AI (1983) Smeshannye Kristally (Mixed crystals). Nauka, Moscow, p 128 (in Russian)
20. Vainshtein BK, Fridkin VM, Indenbom VL (eds) (1994) Modern crystallography, 2nd edn, vol 2. Springer-Verlag, Berlin
21. Thalladi VR et al (1998) J Amer Chem Soc 120:8702
22. Jeffrey JA (1997) An introduction to hydrogen bonding. Oxford University Press
23. Pyykkö P (1997) Chem Rev 97:597
24. Bilton MS, Webster MJ (1972) Chem Soc, Dalton Trans 722
25. Veith M, Agustin D, Huch VJ (2002) Organometal Chem 646:138
26. Burgi H-B, Shklover V (1994) In: Bürgi H-B, Dunitz J D (eds) Structure correlation, vol 1. WCH, Weinheim, p 303 and references therein
27. NIST Chemistry Web Book (2003) http://webbook.nist.gov/chemistry/